bioRxiv preprint doi: https://doi.org/10.1101/2020.05.07.083170; this version posted July 6, 2020. The copyright holder for this preprint (which was not certified by peer review) is the author/funder. All rights reserved. No reuse allowed without permission.

Conjugated activation of myocardial-specific transcription of *Gja5* by a pair of Nkx2-5-Shox2 co-responsive elements

Tianfang Yang[1,*], Zhen Huang[1,2,*], Hua Li[1,2], Linyan Wang[1,3], YiPing Chen[1,‡]

[1]Department of Cell and Molecular Biology
Tulane University
New Orleans, LA 70118, USA

[2]Southern Center for Biomedical Research and Fujian Key Laboratory of Developmental and Neural Biology
College of Life Sciences
Fujian Normal University
Fuzhou, Fujian Province 350108, P.R. China

[3]State Key Laboratory of Oral Diseases
National Clinical Research Center for Oral Diseases
Department of Preventive Dentistry
West China Hospital of Stomatology
Sichuan University
Chengdu, Sichuan Province 610041, P.R.China

*These authors contributed equally to this work

‡Author for correspondence (ychen@tulane.edu)

Running title: A myocardial-specific *Gja5* enhancer

Key-words: *Gja5*, enhancer, myocardium, sinoatrial node, Nkx2-5, Shox2

bioRxiv preprint doi: https://doi.org/10.1101/2020.05.07.083170; this version posted July 6, 2020. The copyright holder for this preprint (which was not certified by peer review) is the author/funder. All rights reserved. No reuse allowed without permission.

Abstract

The sinoatrial node (SAN) is the primary pacemaker in the heart. During cardiogenesis, *Shox2* and *Nkx2-5* are co-expressed in the junction domain of the SAN and regulate pacemaker cell fate through a Shox2-Nkx2-5 antagonism. Cx40 is a marker of working myocardium and an Nkx2-5 transcriptional output antagonized by Shox2, but the underlying regulatory mechanisms remain elusive. Here we characterized a bona fide myocardial-specific *Gja5* (coding gene of Cx40) distal enhancer consisting of a pair of Nkx2-5 and Shox2 co-bound elements in the regulatory region of *Gja5*. Transgenic reporter assays revealed that neither element alone, but the conjugation of both elements together, drives myocardial-specific transcription. Genetic analyses confirmed that the activation of this enhancer depends on Nkx2-5 but is inhibited by Shox2 *in vivo*, and its presence is essential for *Gja5* expression in the myocardium but not the endothelial cells of the heart. Furthermore, chromatin conformation analysis showed an Nkx2-5-dependent loop formation between these two elements and the *Gja5* promoter *in vivo*, indicating that Nkx2-5 bridges the conjugated activation of this enhancer by pairing the two elements to the *Gja5* promoter.

bioRxiv preprint doi: https://doi.org/10.1101/2020.05.07.083170; this version posted July 6, 2020. The copyright holder for this preprint (which was not certified by peer review) is the author/funder. All rights reserved. No reuse allowed without permission.

Introduction

The morphogenesis and physiological maturation of the cardiac conduction system are complicatedly coupled processes, which require a precise spatiotemporal expression of various transcription factors, including Shox2 and Nkx2-5 (Espinoza-Lewis et al., 2009; Hatcher and Basson, 2009; Pashmforoush et al., 2004; van Weerd and Christoffels, 2016). *Nkx2-5* is essential for murine cardiogenesis (Lyons et al., 1995) but its expression was thought to be excluded from the SAN (Espinoza-Lewis et al., 2009), and ectopic expression of Nkx2-5 in the developing SAN inhibits pacemaker cell differentiation (Espinoza-Lewis et al., 2011). In contrast, *Shox2* is essential for SAN development and represses *Nkx2-5* expression in the developing SAN head domain (Espinoza-Lewis et al., 2009; Liu et al., 2014), thus ensuring the absence of Nkx2-5 in the SAN head from the surrounding *Nkx2-5*$^+$ working myocardium. It was recently demonstrated the existence of a *Shox2* and *Nkx2-5* co-expression domain in the developing SAN, genetically dividing the SAN into a *Shox2*$^+$/*Nkx2-5*$^-$ "head" domain and a *Shox2*$^+$/*Nkx2-5*$^+$ "jFunction" domain (Li et al., 2019; Ye et al., 2015). In the *Shox2*$^+$/*Nkx2-5*$^+$ SAN junction domain, a Shox2-Nkx2-5 antagonistic mechanism appears to direct the pacemaker cell fate (Ye et al., 2015).

Gap junction alpha-5 (Gja5)/connexin 40 (Cx40), encoded by *Gja5* in mice, plays a critical role in mediating electrical conduction and diffusion of cellular substances in the heart (Bagwe et al., 2005; de Wit et al., 2003; Simon and McWhorter, 2002). Mutations in *GJA5* in humans are associated with atrial fibrillation (AF) (Bai, 2014; Firouzi et al., 2004; Gollob et al., 2006; Juang et al., 2007) and tetralogy of Fallot (TOF) (Greenway et al., 2009; Guida et al., 2013). During murine cardiogenesis, *Gja5* is selectively expressed in the atrial myocardium, the ventricular conduction system, and the arterial endothelial cells (Beyer et al., 2011; Christoffels and Moorman, 2009; van Weerd and Christoffels, 2016). Cardiac *Gja5* expression depends on Nkx2-5 (Dupays et al., 2005; Espinoza-Lewis et al., 2011; Linhares et al., 2004) but is repressed by Shox2 (Blaschke et al., 2007; Espinoza-Lewis et al., 2009), and is controlled tightly by the Shox2-Nkx2-5 antagonism in the *Nkx2-5*$^+$/*Shox2*$^+$ domains (Li et al., 2019; Ye et al., 2015). However, the underlying mechanisms utilized by Shox2 and Nkx2-5 to control *Gja5* expression remain unknown.

The precise spatiotemporal control of transcriptional networks is critical for cardiac development (Bruneau, 2008; Olson, 2006). Whereas proximal promoters provide a basis for gene transcription, the tissue-specific gene expression is dependent mainly on the interactions

bioRxiv preprint doi: https://doi.org/10.1101/2020.05.07.083170; this version posted July 6, 2020. The copyright holder for this preprint (which was not certified by peer review) is the author/funder. All rights reserved. No reuse allowed without permission.

between existing tissue-specific transcription factors and a variety of regulatory DNA sequences classified as distal enhancers (Levine, 2010; Nord et al., 2013; Visel et al., 2009). In the heart, numerous cardiac-specific distal enhancers have been characterized by comparative genomic analyses searching for evolutionarily conserved elements and genome-wide profiling of active enhancer associated epigenetic marks or co-activator protein binding sites in heart tissues (Blow et al., 2010; Dickel et al., 2016; He et al., 2011; May et al., 2012; Narlikar et al., 2010; Paige et al., 2012; Wamstad et al., 2012). Although the combinatorial binding of cardiac transcription factors at proximal promoters and their physiological significance in transcription regulation have been studied extensively (Bruneau, 2002), the functions of cardiac-specific distal enhancers and how transcription factors regulate them remain largely unexplored.

In this study, we report the characterization of a myocardial-specific *Gja5* distal enhancer, which is formed by a pair of Shox2 and Nkx2-5 co-bound elements (named as *Gja5-S1* and *Gja5-S2*) spaced by a 12-Kb non-coding region downstream of *Gja5*. Neither *Gja5-S1* nor *Gja5-S2* alone, but the conjugation of both elements termed as *Gja5-eh*, displayed robust enhancer activity recapitulating the endogenous *Gja5* expression pattern in the *Nkx2-5*$^{+}$ domain of the developing and adult heart. Genetic analyses showed that the *Gja5-eh* enhancer activity is indeed dependent on Nkx2-5 but is inhibited by Shox2 *in vivo*. Mice bearing the ablation of both *Gja5-S1* and *Gja5-S2* exhibit drastically reduced endogenous *Gja5* expression only in the myocardium but not the arterial endothelial cells, illustrating that these two elements are indispensable for *Gja5* expression specifically in the myocardium *in vivo*. Moreover, chromatin conformation analysis of mouse embryonic hearts showed that both *Gja5-S1* and *Gja5-S2* have frequent contacts with the *Gja5* promoter in an Nkx2-5-dependent manner, indicating that Nkx2-5 bridges the enhancer activation by conjugating *Gja5-S1* and *Gja5-S2* together with the *Gja5* promoter.

bioRxiv preprint doi: https://doi.org/10.1101/2020.05.07.083170; this version posted July 6, 2020. The copyright holder for this preprint (which was not certified by peer review) is the author/funder. All rights reserved. No reuse allowed without permission.

Results and Discussion

Identification of *Gja5-S1* and *Gja5-S2* and generation of *Gja5-eh-LacZ* reporter mouse line

To understand the functional mechanisms underlying the Shox2-Nkx2-5 antagonism that regulates cell fate in the developing SAN, we revisited the genomic profiles of Shox2 and Nkx2-5 ChIP-seq assays on the right atrial tissues of E12.5 mouse embryonic heart, which displayed a substantial genome-wide co-occupancy of Shox2 and Nkx2-5 (Ye et al., 2015). Among the co-binding peaks, two sites (termed *Gja5-S1* and *Gja5-S2*) co-occupied by Shox2 and Nkx2-5 downstream of *Gja5* raised our particular interest (Fig. 1A), because *Gja5* expression has been proven to be regulated by *Shox2* and *Nkx2-5* during SAN development (Li et al., 2019; Ye et al., 2015). *Gja5-S1* locates at around 9-Kb downstream of the *Gja5* coding region, whereas *Gja5-S2* sits downstream of *Gja5-S1* separated by a 12-Kb non-coding sequence. Additional analysis integrating accessible public data showed that *Gja5-S1* and *Gja5-S2* are located in the same topological associated domain (TAD) as *Gja5* (Dixon et al., 2012), and are both marked as putative open chromatin in embryonic hearts but not in any other tissues at the same stage (ENCODE Project Consortium, 2012) (Fig. S1), further suggesting that these two elements may have cardiac-specific enhancer activity.

To assess the enhancer activity of *Gja5-S1* and *Gja5-S2 in vivo*, we initially cloned each of them into a reporter construct containing the *Hsp68* minimal promoter ($Hsp68_{mp}$) and β-galactosidase coding sequence (*LacZ*) (Kothary et al., 1989). However, neither element exhibited enhancer activity in transient transgenic reporter assays (Fig. 1C). We wondered whether the two elements are required to function together, and therefore subsequently conjugated both elements together as a fusion fragment, termed *Gja5-eh*, and generated a reporter construct named *Gja5-eh-LacZ* to test its enhancer activity in transgenic mouse embryos. Strikingly, all the *Gja5-eh-LacZ* transgene-positive embryos (15/15) showed beta-galactosidase (β-gal) activity in the developing heart (Fig. 1B, C). Section immunostaining and X-gal staining further revealed the specific expression of *LacZ* in the myocardium but its absence in the SAN of the transgenic animals, similar to the pattern of endogenous *Gja5* expression (Fig. 1B, D). These observations indicate that both *Gja5-S1* and *Gja5-S2* are required to act together *in cis* to drive cardiac-specific gene transcription. We subsequently generated *Gja5-eh-LacZ* permanent transgenic reporter mouse lines to facilitate further studies.

bioRxiv preprint doi: https://doi.org/10.1101/2020.05.07.083170; this version posted July 6, 2020. The copyright holder for this preprint (which was not certified by peer review) is the author/funder. All rights reserved. No reuse allowed without permission.

Gja5-eh recapitulates endogenous *Gja5* expression in *Nkx2-5*$^{+}$ myocardium

Next, we examined whether the enhancer activity of *Gja5-eh* could faithfully recapitulate the endogenous *Gja5* expression in the developing heart. Since Nkx2-5 binds to *Gja5-S1* and *Gja5-S2* and is essential for *Gja5* expression in the heart (Dupays et al., 2005), we conducted co-immunostaining on Nkx2-5, Cx40, and β-gal in the hearts of *Gja5-eh-LacZ* reporter mice. The results showed co-expression of β-gal and Cx40 in the *Nkx2-5*$^{+}$ myocardium of the ventricle and atrium of *Gja5-eh-LacZ* hearts, not only at the embryonic stage (E12.5) but also at adulthood (P60) (Fig. 2A-D, single-channel images in Fig. S2). Similar to the results seen in the transient transgenic reporter assay, β-gal was not detectable in the *Shox2*$^{+}$ SAN region in contrast to its presence in the adjacent Nkx2-5^{+}/Cx40^{+} atrial myocardium (Fig. 2A, Fig. S2M-P). Notably, we also observed the absence of β-gal in the Nkx2-5^{-}/Cx40^{+} coronary arteries (CA) in contrast to its intense expression in the Nkx2-5^{+}/Cx40^{+} ventricular trabeculae (VT) (Fig. 2D, Fig. S2I-L). Similar observations were found in other developmental stages (data not shown). These results demonstrate that *Gja5-eh* acts as a functional distal enhancer and recapitulates the endogenous *Gja5* expression. However, its enhancer activity is restricted only to the Nkx2-5^{+} myocardium, suggesting a positive role of Nkx2-5 in the activation of the enhancer.

Gja5-eh enhancer activity is dependent on Nkx2-5 but is inhibited by Shox2

To determine whether Nkx2-5 regulates *Gja5-eh* enhancer activity *in vivo*, we compounded *Gja5-eh-LacZ* allele onto an *Nkx2-5*-null background using the *Nkx2-5*^{Cre} knock-in allele (Moses et al., 2001; Ye et al., 2015). As we expected, the enhancer activity of *Gja5-eh* was abolished in the *Nkx2-5*$^{Cre/Cre}$;*Gja5-eh-LacZ* embryonic hearts as compared to controls (Fig. 2E-J), indicating an indispensable role of Nkx2-5 in the activation of *Gja5-eh*. Since Shox2 also binds to *Gja5-S1* and *Gja5-S2* while represses *Gja5* expression in the heart (Espinoza-Lewis et al., 2009; Ye et al., 2015), we next examined whether Shox2 inhibits *Gja5-eh* enhancer activity *in vivo*. To do this, we compounded *Gja5-eh-LacZ* allele with *ROSA26*^{mTmG} and *Shox2*^{Cre} alleles to generate *Shox2*$^{Cre/Cre}$;*Gja5-eh-LacZ*;*ROSA26*^{mTmG} mice, which enabled monitoring of *Gja5-eh* enhancer activity and tracing of *Shox2* lineage in *Shox2*-null background (Sun et al., 2013). In contrast to the absence of β-gal in the *Nkx2-5*$^{+}$ cells derived from the *Shox2* lineage cells that were labeled by mGFP in controls (*Shox2*$^{+/Cre}$;*Gja5-eh-LacZ*;*ROSA26*^{mTmG} (Fig. 2K-N), we observed the presence of *Nkx2-5*$^{+}$/mGFP^{+}/β-gal^{+} cells in the SAN junction, but not the SAN head domain, of

bioRxiv preprint doi: https://doi.org/10.1101/2020.05.07.083170; this version posted July 6, 2020. The copyright holder for this preprint (which was not certified by peer review) is the author/funder. All rights reserved. No reuse allowed without permission.

Shox2$^{Cre/Cre}$;*Gja5-eh-LacZ*;*ROSA26*^{mTmG} mice (Fig. 2O-R), indicating the cell-autonomous ectopic activation of *Gja5-eh* enhancer in the absence of *Shox2*. This result is consistent with the ectopic expression of *Gja5* in the cardiac structures in *Shox2*-null embryos (Espinoza-Lewis et al., 2009; Sun et al., 2015), suggesting that Shox2 suppresses *Gja5* expression by binding to *Gja5-S1* and *Gja5-S2*.

Gja5-S1 and *Gja5-S2* are essential for myocardial *Gja5* expression

To investigate whether *Gja5-S1* and *Gja5-S2* serve as a bona fide distal enhancer that drives endogenous *Gja5* expression, we generated a knockout allele termed *Gja5*$^{\Delta 14}$, which carries a deletion of a 14-Kb region that includes both *Gja5-S1*, *Gja5-S2*, and the sequence between these two sites (Fig. 3A). As a control, we also generated a pseudo-knockout allele termed *Gja5*$^{\Delta 12}$, in which the 12-Kb sequence between *Gja5-S1* and *Gja5-S2* was deleted (Fig. 3B). We subsequently examined and compared the endogenous *Gja5* expression in the hearts of *Gja5*$^{\Delta 14/\Delta 14}$, *Gja5*$^{\Delta 12/\Delta 12}$, as well as wild type mice. Strikingly, we observed that in the perinatal *Gja5*$^{\Delta 14/\Delta 14}$ hearts, Cx40 expression in the atrial and ventricular trabecular myocardium was almost completely abolished but remained unaltered in the coronary arteries (Fig. 3D, G). We also verified by Western blotting the dramatically decreased levels of Cx40 proteins in the atria and ventricles of P0 *Gja5*$^{\Delta 14/\Delta 14}$ mice as compared to *Gja5*$^{+/+}$ controls (Fig. 3I). Further quantification via real-time qPCR (RT-qPCR) showed that the *Gja5* transcription levels remained only 5%±0.2% in the atria and 31%±3.7% in the ventricles of *Gja5*$^{\Delta 14/\Delta 14}$ mice as compared to their counterparts in *Gja5*$^{+/+}$ controls (Fig. 3J). These residual *Gja5* expressions in *Gja5*$^{\Delta 14/\Delta 14}$ groups may largely be contributed by coronary arteries where *Gja5* expression is unaffected. In contrast, immunohistochemical staining revealed indiscernible change in Cx40 expression in both myocardium and coronary arteries in *Gja5*$^{\Delta 12/\Delta 12}$ perinatal hearts as compared to that of *Gja5*$^{+/+}$ mice (Fig. 3E, H). These results demonstrate that *Gja5-S1* and *Gja5-S2* are explicitly required in the myocardium to drive *Gja5* expression, consistent with the specific enhancer activity of *Gja5-eh* in the *Nkx2-5*$^{+}$ myocardium, but not in the *Nkx2-5*$^{-}$ coronary arteries (Fig. S2I-L). Despite the diminished myocardial *Gja5* expression in *Gja5*$^{\Delta 14/\Delta 14}$ hearts, these mice are viable and fertile with no overt phenotype. We subsequently performed surface ECG on adult *Gja5*$^{\Delta 14/\Delta 14}$ mice along with controls but did not find obvious differences between mutants and controls (N = 10 for each genotype, with 5 males and 5 females, data not shown). Indeed,

bioRxiv preprint doi: https://doi.org/10.1101/2020.05.07.083170; this version posted July 6, 2020. The copyright holder for this preprint (which was not certified by peer review) is the author/funder. All rights reserved. No reuse allowed without permission.

Gja5 null mutant mice were viable and fertile, with only minor cardiac physiological abnormalities (prolonged P-wave manifested by ECG) (Bagwe et al., 2005). However, simultaneous loss of *Cx37* and *Gja5*(*Cx40*) results in perinatal lethality with severe vascular defect, indicating that *Gja5* functions importantly but redundantly in the endothelial lineage (Simon and McWhorter, 2002). Therefore, the normal cardiac function of *Gja5*$^{\Delta 14/\Delta 14}$ mice, revealed by ECG, can be explained by the unaffected expression of *Gja5* in the endothelial lineage. Additionally, although a number of mutations within *GJA5* coding regions have been associated with atrial fibrillation, none was reported occurring in the non-coding regulatory element associated with *GJA5* so far. We speculate that the pathogenicity of mutations in *GJA5* may arise from alterations of biochemical properties of the CX40 protein rather than changes in overall CX40 levels. Admittedly, we acknowledge that the physiological consequences of the 14Kb deletion could be tested in more detail by additional methods, such as echocardiography and optical mapping.

An Nkx2-5-dependent interaction between *Gja5-S1*/*Gja5-S2* and the *Gja5* promoter

Recent studies have reported prevalent long-range enhancer-promoter interactions in cardiomyocytes (Montefiori et al., 2018; Rosa-Garrido et al., 2017) and association of disrupted enhancer-promoter looping with cardiac malfunctions (Man et al., 2019). Nkx2-5 was reported to bind to the *Gja5* promoter and upregulate its expression *in vitro* (Linhares et al., 2004), but its functional mechanisms remain elusive. To determine whether *Gja5-S1* and *Gja5-S2* have direct interaction with the *Gja5* promoter and if such interaction requires the presence of Nkx2-5, we performed Chromatin Conformation Capture (3C) (Dekker et al., 2002) assays on E10.5 wild type and *Nkx2-5*$^{Cre/Cre}$ hearts. The results showed that in wild type groups, fragments embracing primer pairs F2+R1 and F4+R1 bore significantly higher relative interaction frequency (RIF) than other primer pairs (Fig. 4A, B), indicating that both *Gja5-S1* and *Gja5-S2* form a strong loop with the *Gja5* promoter. In comparison, the RIF between *Gja5-S1/Gja5-S2* and the *Gja5* promoter of *Nkx2-5*$^{Cre/Cre}$ (*Nkx2-5* null) hearts was significantly reduced (Fig. 4A, B). These results demonstrate an Nkx2-5-dependent loop formation between both *Gja5-S1*/*Gja5-S2* and the *Gja5* promoter, illustrating a critical enhancer-pairing and promoter-docking function of Nkx2-5 in the conjugated activation of *Gja5-S1* and *Gja5-S2*. This bridging function of Nkx2-5 may result from its ability to form homodimers or heterodimerize with other Nkx2 family

bioRxiv preprint doi: https://doi.org/10.1101/2020.05.07.083170; this version posted July 6, 2020. The copyright holder for this preprint (which was not certified by peer review) is the author/funder. All rights reserved. No reuse allowed without permission.

transcription factors (Kasahara et al., 2001). Interestingly, we did not observe the binding peaks of Nkx2-5 to the *Gja5* promoter from our ChIP-seq data (Fig. 1A, Fig. S1), raising the possibility that Nkx2-5 may have different binding preferences at a context-specific manner.

We also looked for consensus binding sites of Nkx2-5 and Shox2 within both *Gja5-S1* and *Gja5-S2* by searching JASPAR-2020, a recently updated database of in vitro DNA binding motifs (Fornes et al., 2019). We found numerous predicted transcription factor binding sites within *Gja5-S1* (Fig. S4) and *Gja5-S2* (Fig. S5). However, there is only one Nkx2-5 binding site (-AACCACTCCAG-) inside *Gja5-S1* but not *Gja5-S2*, while no Shox2 binding site was found. Meanwhile, binding sites of two other NK family transcription factors, Nkx2-3 and Nkx2-8, were found in both *Gja5-S1* (-GCACTTGAG-) and *Gja5-S2* (-CCACTTGAC-). All these three sites share motif -(C/G)CACT(T/C)-, consistent with our Nkx2-5 ChIP-seq results (Ye et al., 2015) and results from another study (He et al., 2011). Our previous studies showed that Shox2 has distinct binding sites among different tissues during organogenesis (Wang et al., 2020; Xu et al., 2019; Ye et al., 2016, 2015), but a common motif is yet to be characterized. The binding preferences of Shox2 may be partially dependent upon other co-factors, such as Hox family transcription factors, as reported previously (Ye et al., 2016).

Based on the work presented here, we propose that *Gja5-S1* and *Gja5-S2* are a pair of Nkx2-5-Shox2 co-responsive elements that act together as a myocardial-specific *Gja5* distal enhancer by interacting with the *Gja5* promoter (Fig. 4C). We acknowledge that as the ChIP-seq and 3C experiments were performed on bulk tissues consisting of both myocardium and SAN, we can not conclude that *Gja5-S1* and *Gja5-S2* are co-bound by both Nkx2-5 and Shox2 simultaneously. One interpretation of the model could be that in the SAN junction, Shox2 competes with Nkx2-5 for binding to these two elements and thus disrupts the interaction of the enhancers with the *Gja5* promoter by keeping the enhancers at a distal status. Another interpretation is that Shox2 and Nkx2-5 form non-functional protein complexes that can not bind to DNA or have diminished DNA binding specificities, since Shox2 and Nkx2-5 have physical interaction *in vitro* (Ye et al., 2015).

While we report that *Gja5-S1* alone does not have enhancer activity (Fig. 1C), a 705-bp *Gja5* enhancer that embraces *Gja5-S1* was reported (Hashimoto et al., 2019). *Gja5-S1* (553-bp) locates in the center of this 705-bp enhancer, flanked by an additional 152-bp sequence (90 bp upstream/62 bp downstream). This additional 152-bp sequence, which contains Hand2 binding

bioRxiv preprint doi: https://doi.org/10.1101/2020.05.07.083170; this version posted July 6, 2020. The copyright holder for this preprint (which was not certified by peer review) is the author/funder. All rights reserved. No reuse allowed without permission.

sites and is enriched in H3K27ac, appears to contribute to the discrepant enhancer activity via H3K27ac deposition recruited by Hand2 (Creyghton et al., 2010; Hashimoto et al., 2019). In contrast, we found that *Gja5-S2* is marked by H3K4me2, H3K4me3, and occupied by CCCTC-binding factor (CTCF) (Fig. S3) (ENCODE Project Consortium, 2012). Both H3K4me2 and H3K4me3 are associated with active transcription (Heintzman et al., 2007; Kim and Buratowski, 2009; Mikkelsen et al., 2007; Santos-Rosa et al., 2002), and CTCF is a critical regulator of enhancer-promoter interactions and chromatin topology (Barrington et al., 2019; Nora et al., 2017; Shin, 2019; Wutz et al., 2017). These distinct histone modifications and binding of chromatin modifiers between *Gja5-S1* and *Gja5-S2* may display complementary actions that contribute to their conjugated activation. Based on the proposed model, we also speculate that a smaller deletion of either *Gja5-S1* or *Gja5-S2* should abolish *Gja5* expression in the myocardium and phenocopy $Gja5^{\Delta 14/\Delta 14}$ mice.

The behaviors of enhancers are multifaceted. During organogenesis, tissue-specific enhancers of the same gene could function redundantly to achieve phenotypic robustness by buffering the loss-of-function mutations of individual enhancers (Frankel et al., 2010; Osterwalder et al., 2018). Strong enhancers may compete for contacting promoters, and enhancers of weak or intermediate strength by themselves may function additively to enhance the expression of the same gene (Bothma et al., 2015). One enhancer may contain multiple binding sites for different transcription factors and is synergistically activated through proximal protein-protein interactions (Ambrosetti et al., 1997; Anderson et al., 2017; Grieder et al., 1997; Hashimoto et al., 2019). Here, our studies show that the nature of enhancers could be even more complicated. This conjugated activation of myocardial-specific activation of *Gja5* by two regulatory elements may represent a novel mechanism for accuracy assurance of tissue-specific gene expression. Although *Gja5-eh* is a recombinant fusion of *Gja5-S1* and *Gja5-S2*, we indeed observed a striking consistency between *Gja5-eh-LacZ* enhancer activity and molecular phenotype of $Gja5^{\Delta 14/\Delta 14}$ mice. We reason that the fusion of *Gja5-S1* and *Gja5-S2* has mimicked their actual close contact at the *Gja5* promoter loci *in vivo*, which makes *Gja5-eh* represent the spatiotemporal behaviors of *Gja5-S1* and *Gja5-S2* precisely. The $Gja5^{\Delta 12}$ allele actually also simulates the fusion of *Gja5-S1* and *Gja5-S2 in situ* and represents their conjugated activation (Fig. 3B, E, H). Collectively, these observations point out a unique pattern of conjugated enhancer activation and provide novel insights into characterization, design, and optimization of

bioRxiv preprint doi: https://doi.org/10.1101/2020.05.07.083170; this version posted July 6, 2020. The copyright holder for this preprint (which was not certified by peer review) is the author/funder. All rights reserved. No reuse allowed without permission.

tissue/lineage-specific enhancers that may benefit biomedical research or therapeutic applications.

bioRxiv preprint doi: https://doi.org/10.1101/2020.05.07.083170; this version posted July 6, 2020. The copyright holder for this preprint (which was not certified by peer review) is the author/funder. All rights reserved. No reuse allowed without permission.

Materials and Methods

Cloning and plasmids

The 553-bp *Gja5-S1* and 594-bp *Gja5-S2* fragments were amplified by PCR, respectively, using primers Gja5-S1-F (5' -AGTCTGATGACAACTTGTGAGAATCG- 3'), Gja5-S1-R (5'- GGGT GACAGTAAGAAATGTCAGGTG- 3'), and Gja5-S2-F (5' -AATGAACAGGAAAGTGGGAG G- 3'), Gja5-S2-R (5'-CAGGGCGGTCAGGCAG- 3'). The 1147 bp fusion fragment *Gja5-eh* was synthesized commercially (Qinglanbiotech.com). Each of the fragments was subsequently cloned into plasmid *hsp68-LacZ* (Kothary et al., 1989) to generate *Gja5-S1-LacZ*, *Gja5-S2-LacZ*, and *Gja5-eh-LacZ* constructs for transient transgenic reporter assays. *Gja5-eh-LacZ* was also used for generating permanent transgenic reporter mouse lines.

Mouse models

The generation and genotyping methods of *Shox2*^{Cre}, *Nkx2-5*^{Cre} and *ROSA26*^{mTmG} mice have been described previously (Moses et al., 2001; Muzumdar et al., 2007; Sun et al., 2013). Generation of transgenic embryos and mice were performed as described previously (Ye et al., 2016). The *Gja5*$^{\Delta 14}$ and *Gja5*$^{\Delta 12}$ alleles were generated by CRISPR/Cas9-mediated genome editing (Wang et al., 2013). Additional details of CRISPR/Cas9-mediated genome editing and transgenesis methods are described in the Supplementary Materials and Methods. All animal work in this study was approved by The Tulane University Institutional Animal Care and Use Committee (IACUC). Sample sizes were empirically determined based on previous experimental procedures (Ye et al., 2016). Mouse embryos were excluded from further analysis only if they did not carry alleles of interest.

Histology, immunohistochemistry, and X-gal staining

Hearts were harvested from properly euthanized mice or staged embryos, fixed in ice-cold 4% paraformaldehyde (PFA) overnight at 4□, dehydrated through gradient ethanol, cleared in xylene, embedded in paraffin, and sectioned at 5μm for immunostaining as described previously (Li et al., 2019). The primary antibodies used in this study were: anti-Hcn4 (ab32675, Abcam; 1:200), anti-Nkx2-5 (AF2444, Novus Biologicals; 1:200), anti-Cx40 (Cx40-A; Alpha Diagnostic International; 1:200), anti-GFP (sc-9996, Santa Cruz Biotechnology; 1:200), anti-β-galactosidase (ab9361, Abcam; 1:200). The secondary antibodies were used at 1:1000 and all from Jackson

bioRxiv preprint doi: https://doi.org/10.1101/2020.05.07.083170; this version posted July 6, 2020. The copyright holder for this preprint (which was not certified by peer review) is the author/funder. All rights reserved. No reuse allowed without permission.

ImmunoResearch: donkey anti-goat (705-545-147), donkey anti-mouse (705-585-151), donkey anti-rabbit (711-585-152, 711-545-152), donkey anti-rat (712-585-153), donkey anti-chicken (703-606-155).

For whole-mount X-gal staining, staged embryos were fixed with freshly-prepared, ice-cold 2% PFA and 0.2% glutaraldehyde in PBS for 1 hour at 4□, rinsed with staining solution (5mM potassium ferricyanide, 5mM potassium ferrocyanide, 2mM $MgCl_2$, 0.01% sodium deoxycholate, and 0.02% IGEPAL CA-630), followed by addition of X-gal stock solution (40mg/ml in dimethylformamide) at 1:40. For section X-gal staining, fixed embryos were dehydrated through gradient sucrose/OCT, embedded in OCT, cryo-sectioned at 10μm, and stained for X-gal as described above.

Western Blot and real-time quantitative PCR (RT-qPCR)

P0 pups of wild type and *Gja5*$^{\Delta 14/\Delta 14}$ mice were euthanized by decapitation. Hearts were then isolated, and atria were separated from ventricles. Samples from about 20 pups of each genotype were pooled, homogenized, and subjected to protein extraction or RNA extraction followed by cDNA preparation, as previously described (Li et al., 2019; Ye et al., 2015). For Western Blot, the following primary antibodies were used: anti-Cx40 (Cx40-A; Alpha Diagnostic International; 1:2000), anti-GAPDH (2118S; Cell Signaling Technology; 1:2000). The secondary antibody used was: IRDye® 800CW Donkey anti-Rabbit (926-32213; LI-COR; 1:10000). For RT-qPCR, the following primers were used: *Gja5* (F, 5’ -GGTCCACAAGCACTCCACAG- 3’; R, 5′-CTG AATGGTATCGCACCGGAA- 3′), *Gapdh* (F, 5’ -ATCAAGAAGGTGGTGAAGCAG- 3’; R, 5′ -GAGTGGGAGTTGCTGTTGAAGT- 3′).

Chromatin Conformation Capture (3C) assays

Briefly, embryonic hearts were dissected under a microscope, minced into small pieces and digested with Accutase (Invitrogen 00-4555-56) at 37□ for about 20 minutes, passed through a 70μm cell strainer, followed by formaldehyde fixation and quenched with glycine. The cells were then cryoprotected at -80□. 1×10^7 cells of each genotype (about 30 wild type embryos or 50 *Nkx2-5*$^{Cre/Cre}$ embryos) were pooled for each 3C library preparation following standard procedures (Cope and Fraser, 2009). The relative interaction frequency (RIF) of each fragment of interest was measured by RT-qPCR, as described previously (Li et al., 2019). Primer details

bioRxiv preprint doi: https://doi.org/10.1101/2020.05.07.083170; this version posted July 6, 2020. The copyright holder for this preprint (which was not certified by peer review) is the author/funder. All rights reserved. No reuse allowed without permission.

are as follows: F1 (5' -GCCAAGGCCCTCAAGGTGA- 3'), F2 (5' -GGAGGGATTTGATATG AATGTAAGCACTG- 3'), F3 (5' -ATTCATGTAAGAGGGTCTGATCTCCAG- 3'), F4 (5' -A CAACCTTATCTCCAAACCTTTGCTC- 3'), R1 (5' -CCATTCCCTTTAGGACGGTTACCTT C- 3'), R2 (5' -CATGGACTGACCTCATTGGAGTG- 3'), R3 (5' -GGGAGGGATTCAGGAC ATGTTG- 3').

Statistical analysis

All experiments were repeated at least three times to ensure scientific reproducibility. Quantification results are presented as mean±s.e.m., and statistical analysis was conducted using Student's *t*-test in a GraphPad Prism 6 software. $P<0.05$ was considered significant.

Acknowledgments

We thank Mrs. Ann Mullin at the Tulane Transgenic Animal Core Facility for assistance with the generation of genetically modified mice.

Competing interests

The authors declare no competing or financial interests.

Author contributions

Conceptualization: Y.C., T.Y.; Methodology: Y.C., T.Y., Z.H.; Validation: Y.C., T.Y.; Formal analysis: T.Y., Z.H., H.L.; Investigation: T.Y., Z.H., H.L., L.W.; Resources: Y.C.; Data curation: Y.C., T.Y.; Writing - original draft: T.Y.; Writing - review & editing: Y.C.; Visualization: T.Y.; Supervision: Y.C.; Project administration: Y.C.; Funding acquisition: Y.C.

Funding

We acknowledge financial support by the National Institutes of Health (R01HL136326 to Y.C.) and an American Heart Association (AHA) Predoctoral Fellowship (20PRE35040002 to T.Y.). H.L. and Z.H. were supported in part by fellowships from Fujian Normal University, and L.W. received a fellowship from the China Scholarship Council.

bioRxiv preprint doi: https://doi.org/10.1101/2020.05.07.083170; this version posted July 6, 2020. The copyright holder for this preprint (which was not certified by peer review) is the author/funder. All rights reserved. No reuse allowed without permission.

References

Ambrosetti, D.C., Basilico, C., Dailey, L., 1997. Synergistic activation of the fibroblast growth factor 4 enhancer by Sox2 and Oct-3 depends on protein-protein interactions facilitated by a specific spatial arrangement of factor binding sites. Mol. Cell. Biol. 17, 6321–6329. https://doi.org/10.1128/mcb.17.11.6321

Anderson, C.M., Hu, J., Thomas, R., Gainous, T.B., Celona, B., Sinha, T., Dickel, D.E., Heidt, A.B., Xu, S.M., Bruneau, B.G., Pollard, K.S., Pennacchio, L.A., Black, B.L., 2017. Cooperative activation of cardiac transcription through myocardin bridging of paired MEF2 sites. Development 144, 1235–1241. https://doi.org/10.1242/dev.138487

Bagwe, S., Berenfeld, O., Vaidya, D., Morley, G.E., Jalife, J., 2005. Altered Right Atrial Excitation and Propagation in Connexin40 Knockout Mice. Circulation 112, 2245–2253. https://doi.org/10.1161/CIRCULATIONAHA.104.527325

Bai, D., 2014. Atrial fibrillation-linked *GJA5* /connexin40 mutants impaired gap junctions via different mechanisms. FEBS Lett. 588, 1238–1243. https://doi.org/10.1016/j.febslet.2014.02.064

Barrington, C., Georgopoulou, D., Pezic, D., Varsally, W., Herrero, J., Hadjur, S., 2019. Enhancer accessibility and CTCF occupancy underlie asymmetric TAD architecture and cell type specific genome topology. Nat. Commun. 10, 1–14. https://doi.org/10.1038/s41467-019-10725-9

Beyer, S., Kelly, R.G., Miquerol, L., 2011. Inducible Cx40-Cre expression in the cardiac conduction system and arterial endothelial cells. Genesis 49, 83–91. https://doi.org/10.1002/dvg.20687

Blaschke, R.J., Hahurij, N.D., Kuijper, S., Just, S., Wisse, L.J., Deissler, K., Maxelon, T., Anastassiadis, K., Spitzer, J., Hardt, S.E., Scho□ler, H., Feitsma, H., Rottbauer, W., Blum, M., Meijlink, F., Rappold, G., Gittenberger-de Groot, A.C., 2007. Targeted Mutation Reveals Essential Functions of the Homeodomain Transcription Factor *Shox2* in Sinoatrial and Pacemaking Development. Circulation 115, 1830–1838. https://doi.org/10.1161/CIRCULATIONAHA.106.637819

bioRxiv preprint doi: https://doi.org/10.1101/2020.05.07.083170; this version posted July 6, 2020. The copyright holder for this preprint (which was not certified by peer review) is the author/funder. All rights reserved. No reuse allowed without permission.

Blow, M.J., McCulley, D.J., Li, Z., Zhang, T., Akiyama, J.A., Holt, A., Plajzer-Frick, I., Shoukry, M., Wright, C., Chen, F., Afzal, V., Bristow, J., Ren, B., Black, B.L., Rubin, E.M., Visel, A., Pennacchio, L.A., 2010. ChIP-seq identification of weakly conserved heart enhancers. Nat. Genet. 42, 806–812. https://doi.org/10.1038/ng.650

Bothma, J.P., Garcia, H.G., Ng, S., Perry, M.W., Gregor, T., Levine, M., 2015. Enhancer additivity and non-additivity are determined by enhancer strength in the Drosophila embryo. Elife 4, e07956. https://doi.org/10.7554/eLife.07956.001

Bruneau, B.G., 2008. The developmental genetics of congenital heart disease. Nature 451, 943–948. https://doi.org/10.1038/nature06801

Bruneau, B.G., 2002. Transcriptional Regulation of Vertebrate Cardiac Morphogenesis. Circ Res. 90, 509–19. https://doi.org/doi: 10.1161/01.res.0000013072.51957.b7.

Christoffels, V.M., Moorman, A.F.M., 2009. Development of the cardiac conduction system: why are some regions of the heart more arrhythmogenic than others? Circ. Arrhythm. Electrophysiol. 2, 195–207. https://doi.org/10.1161/CIRCEP.108.829341

Cope, N.F., Fraser, P., 2009. Chromosome conformation capture. Cold Spring Harb. Protoc. 4. https://doi.org/10.1101/pdb.prot5137

Creyghton, M.P., Cheng, A.W., Welstead, G.G., Kooistra, T., Carey, B.W., Steine, E.J., Hanna, J., Lodato, M.A., Frampton, G.M., Sharp, P.A., Boyer, L.A., Young, R.A., Jaenisch, R., 2010. Histone H3K27ac separates active from poised enhancers and predicts developmental state. Proc. Natl. Acad. Sci. U. S. A. 107, 21931–6. https://doi.org/10.1073/pnas.1016071107

de Wit, C., Roos, F., Bolz, S.-S., Pohl, U., 2003. Lack of vascular connexin 40 is associated with hypertension and irregular arteriolar vasomotion. Physiol. Genomics 13, 169–177. https://doi.org/10.1152/physiolgenomics.00169.2002

Dekker, J., Rippe, K., Dekker, M., Kleckner, N., 2002. Capturing chromosome conformation. Science, 295, 1306–1311. https://doi.org/10.1126/science.1067799

Dickel, D.E., Barozzi, I., Zhu, Y., Fukuda-Yuzawa, Y., Osterwalder, M., Mannion, B.J., May, D., Spurrell, C.H., Plajzer-Frick, I., Pickle, C.S., Lee, E., Garvin, T.H., Kato, M., Akiyama, J.A.,

bioRxiv preprint doi: https://doi.org/10.1101/2020.05.07.083170; this version posted July 6, 2020. The copyright holder for this preprint (which was not certified by peer review) is the author/funder. All rights reserved. No reuse allowed without permission.

Afzal, V., Lee, A.Y., Gorkin, D.U., Ren, B., Rubin, E.M., Visel, A., Pennacchio, L.A., 2016. Genome-wide compendium and functional assessment of in vivo heart enhancers. Nat. Commun. 7, 1–13. https://doi.org/10.1038/ncomms12923

Dixon, J.R., Selvaraj, S., Yue, F., Kim, A., Li, Y., Shen, Y., Hu, M., Liu, J.S., Ren, B., 2012. Topological domains in mammalian genomes identified by analysis of chromatin interactions. Nature 485, 376–380. https://doi.org/10.1038/nature11082

Dupays, L., Jarry-Guichard, T., Mazurais, D., Calmels, T., Izumo, S., Gros, D., Théveniau-Ruissy, M., 2005. Dysregulation of connexins and inactivation of NFATc1 in the cardiovascular system of Nkx2-5 null mutants. J. Mol. Cell. Cardiol. 38, 787–798. https://doi.org/10.1016/j.yjmcc.2005.02.021

ENCODE Project Consortium, 2012. An integrated encyclopedia of DNA elements in the human genome. Nature 489, 57–74. https://doi.org/10.1038/nature11247

Espinoza-Lewis, R.A., Liu, H., Sun, C., Chen, C., Jiao, K., Chen, Y., 2011. Ectopic expression of Nkx2.5 suppresses the formation of the sinoatrial node in mice. Dev. Biol. 356, 359–369. https://doi.org/10.1016/J.YDBIO.2011.05.663

Espinoza-Lewis, R.A., Yu, L., He, F., Liu, H., Tang, R., Shi, J., Sun, X., Martin, J.F., Wang, D., Yang, J., Chen, Y., 2009. Shox2 is essential for the differentiation of cardiac pacemaker cells by repressing Nkx2-5. Dev. Biol. 327, 376–385. https://doi.org/10.1016/j.ydbio.2008.12.028

Firouzi, M., Ramanna, H., Kok, B., Jongsma, H.J., Koeleman, B.P.C., Doevendans, P.A., Groenewegen, W.A., Hauer, R.N.W., 2004. Association of human connexin40 gene polymorphisms with atrial vulnerability as a risk factor for idiopathic atrial fibrillation. Circ. Res. 95, e29-33. https://doi.org/10.1161/01.RES.0000141134.64811.0a

Fornes, O., Castro-Mondragon, J.A., Khan, A., Van Der Lee, R., Zhang, X., Richmond, P.A., Modi, B.P., Correard, S., Gheorghe, M., Baranaší, D., Baranaší, B., Santana-Garcia, W., Tan, G., Chèneby, J., Chèneby, C., Ballester, B., Ois Parcy, F., Sandelin, A., Lenhard, B., Wasserman, W.W., Mathelier, A., 2019. JASPAR 2020: update of the open-access database

bioRxiv preprint doi: https://doi.org/10.1101/2020.05.07.083170; this version posted July 6, 2020. The copyright holder for this preprint (which was not certified by peer review) is the author/funder. All rights reserved. No reuse allowed without permission.

of transcription factor binding profiles. Nucleic Acids Res. 48, 87–92. https://doi.org/10.1093/nar/gkz1001

Frankel, N., Davis, G.K., Vargas, D., Wang, S., Payre, F., Stern, D.L., 2010. Phenotypic robustness conferred by apparently redundant transcriptional enhancers. Nature 466, 490–493. https://doi.org/10.1038/nature09158

Gollob, M.H., Jones, D.L., Krahn, A.D., Danis, L., Gong, X.Q., Shao, Q., Liu, X., Veinot, J.P., Tang, A.S.L., Stewart, A.F.R., Tesson, F., Klein, G.J., Yee, R., Skanes, A.C., Guiraudon, G.M., Ebihara, L., Bai, D., 2006. Somatic mutations in the connexin 40 gene (GJA5) in atrial fibrillation. N. Engl. J. Med. 354, 2677–2688. https://doi.org/10.1056/NEJMoa052800

Greenway, S.C., Pereira, A.C., Lin, J.C., Depalma, S.R., Israel, S.J., Mesquita, S.M., Ergul, E., Conta, J.H., Korn, J.M., McCarroll, S.A., Gorham, J.M., Gabriel, S., Altshuler, D.M., De Lourdes Quintanilla-Dieck, M., Artunduaga, M.A., Eavey, R.D., Plenge, R.M., Shadick, N.A., Weinblatt, M.E., De Jager, P.L., Hafler, D.A., Breitbart, R.E., Seidman, J.G., Seidman, C.E., 2009. De novo copy number variants identify new genes and loci in isolated sporadic tetralogy of Fallot. Nat. Genet. 41, 931–935. https://doi.org/10.1038/ng.415

Grieder, N.C., Marty, T., Ryoo, H.-D., Mann, R.S., Affolter, M., 1997. Synergistic activation of a Drosophila enhancer by HOM/EXD and DPP signaling. EMBO J. 16, 7402–7410. https://doi.org/10.1093/emboj/16.24.7402

Guida, V., Ferese, R., Rocchetti, M., Bonetti, M., Sarkozy, A., Cecchetti, S., Gelmetti, V., Lepri, F., Copetti, M., Lamorte, G., Cristina Digilio, M., Marino, B., Zaza, A., Den Hertog, J., Dallapiccola, B., De Luca, A., 2013. A variant in the carboxyl-terminus of connexin 40 alters GAP junctions and increases risk for tetralogy of Fallot. Eur. J. Hum. Genet. 21, 69–75. https://doi.org/10.1038/ejhg.2012.109

Hashimoto, H., Wang, Z., Garry, G.A., Malladi, V.S., Botten, G.A., Ye, W., Zhou, H., Osterwalder, M., Dickel, D.E., Visel, A., Liu, N., Bassel-Duby, R., Olson, E.N., 2019. Cardiac Reprogramming Factors Synergistically Activate Genome-wide Cardiogenic Stage-Specific Enhancers. Cell Stem Cell 25, 69-86.e5. https://doi.org/10.1016/j.stem.2019.03.022

bioRxiv preprint doi: https://doi.org/10.1101/2020.05.07.083170; this version posted July 6, 2020. The copyright holder for this preprint (which was not certified by peer review) is the author/funder. All rights reserved. No reuse allowed without permission.

Hatcher, C.J., Basson, C.T., 2009. Specification of the Cardiac Conduction System by Transcription Factors. Circ. Res. 105, 620–630. https://doi.org/10.1161/CIRCRESAHA.109.204123

He, A., Kong, S.W., Ma, Q., Pu, W.T., 2011. Co-occupancy by multiple cardiac transcription factors identifies transcriptional enhancers active in heart. Proc. Natl. Acad. Sci. U. S. A. 108, 5632–5637. https://doi.org/10.1073/pnas.1016959108

Heintzman, N.D., Stuart, R.K., Hon, G., Fu, Y., Ching, C.W., Hawkins, R.D., Barrera, L.O., Van Calcar, S., Qu, C., Ching, K.A., Wang, W., Weng, Z., Green, R.D., Crawford, G.E., Ren, B., 2007. Distinct and predictive chromatin signatures of transcriptional promoters and enhancers in the human genome. Nat. Genet. 39, 311–318. https://doi.org/10.1038/ng1966

Juang, J.M., Chern, Y.R., Tsai, C.T., Chiang, F.T., Lin, J.L., Hwang, J.J., Hsu, K.L., Tseng, C. Den, Tseng, Y.Z., Lai, L.P., 2007. The association of human connexin 40 genetic polymorphisms with atrial fibrillation. Int. J. Cardiol. 116, 107–112. https://doi.org/10.1016/j.ijcard.2006.03.037

Kasahara, H., Usheva, A., Ueyama, T., Aoki, H., Horikoshi, N., Izumo, S., 2001. Characterization of Homo- and Heterodimerization of Cardiac Csx/Nkx2.5 Homeoprotein. J. Biol. Chem. 276, 4570–4580. https://doi.org/10.1074/jbc.M004995200

Kim, T.S., Buratowski, S., 2009. Dimethylation of H3K4 by Set1 Recruits the Set3 Histone Deacetylase Complex to 5′ Transcribed Regions. Cell 137, 259–272. https://doi.org/10.1016/j.cell.2009.02.045

Kothary, R., Clapoff, S., Darling, S., Perry, M.D., Moran, L.A., Rossant, J., 1989. Inducible expression of an hsp68-lacZ hybrid gene in transgenic mice. Development 105, 707–714.

Levine, M., 2010. Transcriptional enhancers in animal development and evolution. Curr. Biol. 20, R754–R763. https://doi.org/10.1016/j.cub.2010.06.070

Li, H., Li, D., Wang, Y., Huang, Z., Xu, J., Yang, T., Wang, L., Tang, Q., Cai, C.-L., Huang, H., Zhang, Y., Chen, Y., 2019. Nkx2-5 defines a subpopulation of pacemaker cells and is essential for the physiological function of the sinoatrial node in mice. Development 146, dev178145. https://doi.org/10.1242/dev.178145

bioRxiv preprint doi: https://doi.org/10.1101/2020.05.07.083170; this version posted July 6, 2020. The copyright holder for this preprint (which was not certified by peer review) is the author/funder. All rights reserved. No reuse allowed without permission.

Linhares, V.L.F., Almeida, N.A.S., Menezes, D.C., Elliott, D.A., Lai, D., Beyer, E.C., Campos De Carvalho, A.C., Costa, M.W., 2004. Transcriptional regulation of the murine Connexin40 promoter by cardiac factors Nkx2-5, GATA4 and Tbx5. Cardiovasc. Res. 64, 402–411. https://doi.org/10.1016/j.cardiores.2004.09.021

Liu, H., Chen, C., Ye, W., Espinoza□Lewis, R.A., Hu, X., Zhang, Y., Chen, Y., 2014. Phosphorylation of Shox2 Is Required for Its Function to Control Sinoatrial Node Formation. J. Am. Heart Assoc. 3, e000796. https://doi.org/10.1161/JAHA.114.000796

Lyons, I., Parsons, L.M., Hartley, L., Li, R., Andrews, J.E., Robb, L., Harvey, R.P., 1995. Myogenic and morphogenetic defects in the heart tubes of murine embryos lacking the homeo box gene Nkx2-5. Genes Dev. 9, 1654–66. https://doi.org/10.1101/GAD.9.13.1654

Man, J.C.K., Mohan, R.A., Boogaard, M. van den, Hilvering, C.R.E., Jenkins, C., Wakker, V., Bianchi, V., Laat, W. de, Barnett, P., Boukens, B.J., Christoffels, V.M., 2019. An enhancer cluster controls gene activity and topology of the SCN5A-SCN10A locus in vivo. Nat. Commun. 10, 1–15. https://doi.org/10.1038/s41467-019-12856-5

May, D., Blow, M.J., Kaplan, T., McCulley, D.J., Jensen, B.C., Akiyama, J.A., Holt, A., Plajzer-Frick, I., Shoukry, M., Wright, C., Afzal, V., Simpson, P.C., Rubin, E.M., Black, B.L., Bristow, J., Pennacchio, L.A., Visel, A., 2012. Large-scale discovery of enhancers from human heart tissue. Nat. Genet. 44, 89–93. https://doi.org/10.1038/ng.1006

Mikkelsen, T.S., Ku, M., Jaffe, D.B., Issac, B., Lieberman, E., Giannoukos, G., Alvarez, P., Brockman, W., Kim, T.K., Koche, R.P., Lee, W., Mendenhall, E., O'Donovan, A., Presser, A., Russ, C., Xie, X., Meissner, A., Wernig, M., Jaenisch, R., Nusbaum, C., Lander, E.S., Bernstein, B.E., 2007. Genome-wide maps of chromatin state in pluripotent and lineage-committed cells. Nature 448, 553–560. https://doi.org/10.1038/nature06008

Montefiori, L.E., Sobreira, D.R., Sakabe, N.J., Aneas, I., Joslin, A.C., Hansen, G.T., Bozek, G., Moskowitz, I.P., McNally, E.M., Nóbrega, M.A., 2018. A promoter interaction map for cardiovascular disease genetics. Elife 7. https://doi.org/10.7554/eLife.35788

bioRxiv preprint doi: https://doi.org/10.1101/2020.05.07.083170; this version posted July 6, 2020. The copyright holder for this preprint (which was not certified by peer review) is the author/funder. All rights reserved. No reuse allowed without permission.

Moses, K.A., Demayo, F., Braun, R.M., Reecy, J.L., Schwartz, R.J., 2001. Embryonic expression of an Nkx2-5/Cre gene using ROSA26 reporter mice. Genesis 31, 176–180. https://doi.org/10.1002/gene.10022

Muzumdar, M.D., Tasic, B., Miyamichi, K., Li, N., Luo, L., 2007. A global double-fluorescent cre reporter mouse. Genesis 45, 593–605. https://doi.org/10.1002/dvg.20335

Narlikar, L., Sakabe, N.J., Blanski, A.A., Arimura, F.E., Westlund, J.M., Nobrega, M.A., Ovcharenko, I., 2010. Genome-wide discovery of human heart enhancers. Genome Res. 20, 381–392. https://doi.org/10.1101/gr.098657.109

Nora, E.P., Goloborodko, A., Valton, A.L., Gibcus, J.H., Uebersohn, A., Abdennur, N., Dekker, J., Mirny, L.A., Bruneau, B.G., 2017. Targeted Degradation of CTCF Decouples Local Insulation of Chromosome Domains from Genomic Compartmentalization. Cell 169, 930-944.e22. https://doi.org/10.1016/j.cell.2017.05.004

Nord, A.S., Blow, M.J., Attanasio, C., Akiyama, J.A., Holt, A., Hosseini, R., Phouanenavong, S., Plajzer-Frick, I., Shoukry, M., Afzal, V., Rubenstein, J.L.R., Rubin, E.M., Pennacchio, L.A., Visel, A., 2013. Rapid and pervasive changes in genome-wide enhancer usage during mammalian development. Cell 155, 1521–1531. https://doi.org/10.1016/j.cell.2013.11.033

Olson, E.N., 2006. Gene regulatory networks in the evolution and development of the heart. Science (80-.). 313, 1922–1927. https://doi.org/10.1126/science.1132292

Osterwalder, M., Barozzi, I., Tissiéres, V., Fukuda-Yuzawa, Y., Mannion, B.J., Afzal, S.Y., Lee, E.A., Zhu, Y., Plajzer-Frick, I., Pickle, C.S., Kato, M., Garvin, T.H., Pham, Q.T., Harrington, A.N., Akiyama, J.A., Afzal, V., Lopez-Rios, J., Dickel, D.E., Visel, A., Pennacchio, L.A., 2018. Enhancer redundancy provides phenotypic robustness in mammalian development. Nature 554, 239–243. https://doi.org/10.1038/nature25461

Paige, S.L., Thomas, S., Stoick-Cooper, C.L., Wang, H., Maves, L., Sandstrom, R., Pabon, L., Reinecke, H., Pratt, G., Keller, G., Moon, R.T., Stamatoyannopoulos, J., Murry, C.E., 2012. A temporal chromatin signature in human embryonic stem cells identifies regulators of cardiac development. Cell 151, 221–232. https://doi.org/10.1016/j.cell.2012.08.027

bioRxiv preprint doi: https://doi.org/10.1101/2020.05.07.083170; this version posted July 6, 2020. The copyright holder for this preprint (which was not certified by peer review) is the author/funder. All rights reserved. No reuse allowed without permission.

Pashmforoush, M., Lu, J.T., Chen, H., Amand, T.S., Kondo, R., Pradervand, S., Evans, S.M., Clark, B., Feramisco, J.R., Giles, W., Ho, S.Y., Benson, D.W., Silberbach, M., Shou, W., Chien, K.R., 2004. Nkx2-5 pathways and congenital heart disease; loss of ventricular myocyte lineage specification leads to progressive cardiomyopathy and complete heart block. Cell 117, 373–86.

Rosa-Garrido, M., Chapski, D.J., Schmitt, A.D., Kimball, T.H., Karbassi, E., Monte, E., Balderas, E., Pellegrini, M., Shih, T.T., Soehalim, E., Liem, D., Ping, P., Galjart, N.J., Ren, S., Wang, Y., Ren, B., Vondriska, T.M., 2017. High-resolution mapping of chromatin conformation in cardiac myocytes reveals structural remodeling of the epigenome in heart failure. Circulation 136, 1613–1625. https://doi.org/10.1161/CIRCULATIONAHA.117.029430

Santos-Rosa, H., Schneider, R., Bannister, A.J., Sherriff, J., Bernstein, B.E., Emre, N.C.T., Schreiber, S.L., Mellor, J., Kouzarides, T., 2002. Active genes are tri-methylated at K4 of histone H3. Nature 419, 407–411. https://doi.org/10.1038/nature01080

Shin, H.Y., 2019. The structural and functional roles of CTCF in the regulation of cell type-specific and human disease-associated super-enhancers. Genes and Genomics 41, 257–265. https://doi.org/10.1007/s13258-018-0768-z

Simon, A.M., McWhorter, A.R., 2002. Vascular abnormalities in mice lacking the endothelial gap junction proteins connexin37 and connexin40. Dev. Biol. 251, 206–220. https://doi.org/10.1006/dbio.2002.0826

Sun, C., Yu, D., Ye, W., Liu, C., Gu, S., Sinsheimer, N.R., Song, Z., Li, X., Chen, C., Song, Y., Wang, S., Schrader, L., Chen, Y.P., 2015. The short stature homeobox 2 (Shox2)-bone morphogenetic protein (BMP) pathway regulates dorsal mesenchymal protrusion development and its temporary function as a pacemaker during cardiogenesis. J. Biol. Chem. 290, 2007–2023. https://doi.org/10.1074/jbc.M114.619007

Sun, C., Zhang, T., Liu, C., Gu, S., Chen, Y., 2013. Generation of Shox2-Cre allele for tissue specific manipulation of genes in the developing heart, palate, and limb. Genesis 51, 515–522. https://doi.org/10.1002/dvg.22397

bioRxiv preprint doi: https://doi.org/10.1101/2020.05.07.083170; this version posted July 6, 2020. The copyright holder for this preprint (which was not certified by peer review) is the author/funder. All rights reserved. No reuse allowed without permission.

van Weerd, J.H., Christoffels, V.M., 2016. The formation and function of the cardiac conduction system. Development 143, 197–210. https://doi.org/10.1242/dev.124883

Visel, A., Rubin, E.M., Pennacchio, L.A., 2009. Genomic views of distant-acting enhancers. Nature 461, 199–205. https://doi.org/10.1038/nature08451

Wamstad, J.A., Alexander, J.M., Truty, R.M., Shrikumar, A., Li, F., Eilertson, K.E., Ding, H., Wylie, J.N., Pico, A.R., Capra, J.A., Erwin, G., Kattman, S.J., Keller, G.M., Srivastava, D., Levine, S.S., Pollard, K.S., Holloway, A.K., Boyer, L.A., Bruneau, B.G., 2012. Dynamic and coordinated epigenetic regulation of developmental transitions in the cardiac lineage. Cell 151, 206–220. https://doi.org/10.1016/j.cell.2012.07.035

Wang, H., Yang, H., Shivalila, C.S., Dawlaty, M.M., Cheng, A.W., Zhang, F., Jaenisch, R., 2013. One-step generation of mice carrying mutations in multiple genes by CRISPR/cas-mediated genome engineering. Cell 153, 910–918. https://doi.org/10.1016/j.cell.2013.04.025

Wang, L., Tang, Q., Xu, J., Li, H., Yang, T., Li, L., Machon, O., Hu, T., Chen, Y.P., 2020. The transcriptional regulator MEIS2 sets up the ground state for palatal osteogenesis in mice. J. Biol. Chem. 295, 5449–5460. https://doi.org/10.1074/jbc.RA120.012684

Wutz, G., Várnai, C., Nagasaka, K., Cisneros, D.A., Stocsits, R.R., Tang, W., Schoenfelder, S., Jessberger, G., Muhar, M., Hossain, M.J., Walther, N., Koch, B., Kueblbeck, M., Ellenberg, J., Zuber, J., Fraser, P., Peters, J., 2017. Topologically associating domains and chromatin loops depend on cohesin and are regulated by CTCF, WAPL, and PDS5 proteins. EMBO J. 36, 3573–3599. https://doi.org/10.15252/embj.201798004

Xu, J., Wang, L., Li, H., Yang, T., Zhang, Y., Hu, T., Huang, Z., Chen, Y.P., 2019. Shox2 regulates osteogenic differentiation and pattern formation during hard palate development in mice. J. Biol. Chem. 294, 18294–18305. https://doi.org/10.1074/jbc.RA119.008801

Ye, W., Song, Y., Huang, Z., Osterwalder, M., Ljubojevic, A., Xu, J., Bobick, B., Abassah-Oppong, S., Ruan, N., Shamby, R., Yu, D., Zhang, L., Cai, C.-L., Visel, A., Zhang, Y., Cobb, J., Chen, Y., 2016. A unique stylopod patterning mechanism by Shox2-controlled osteogenesis. Development 143, 2548–2560. https://doi.org/10.1242/DEV.138750

bioRxiv preprint doi: https://doi.org/10.1101/2020.05.07.083170; this version posted July 6, 2020. The copyright holder for this preprint (which was not certified by peer review) is the author/funder. All rights reserved. No reuse allowed without permission.

Ye, W., Wang, J., Song, Y., Yu, D., Sun, C., Liu, C., Chen, F., Zhang, Y., Wang, F., Harvey, R.P., Schrader, L., Martin, J.F., Chen, Y., 2015. A common Shox2-Nkx2-5 antagonistic mechanism primes the pacemaker cell fate in the pulmonary vein myocardium and sinoatrial node. Development 142, 2521–2532. https://doi.org/10.1242/dev.120220

bioRxiv preprint doi: https://doi.org/10.1101/2020.05.07.083170; this version posted July 6, 2020. The copyright holder for this preprint (which was not certified by peer review) is the author/funder. All rights reserved. No reuse allowed without permission.

Figure Legends

Figure 1

Figure 1. Identification of *Gja5-S1* and *Gja5-S2* and generation of *Gja5-eh-LacZ* reporter mice.

(A) Schematic overview of ChIP-seq data collection, visualization, and identification of *Gja5-S1* and *Gja5-S2*, and generation of *Gja5-eh-LacZ* transgenic construct. (B) Whole-mount X-gal staining and section immunostaining of β-galactosidase of E10.5, E11.5 and E12.5 *Gja5-eh-LacZ* embryos. (C) Schematic diagram summarizing the reporter constructs of *Gja5-S1*, *Gja5-S2*, and *Gja5-eh*. The left column indicates the design of each construct. The middle column indicates the number of transgene-positive F0 embryos as a fraction of the total number of F0 embryos. The right column indicates the number of F0 embryos showing cardiac-specific X-gal activity as a fraction of the total number of transgene-positive F0 embryos. (D) X-gal staining on a cryo-sectioned E10.5 *Gja5-eh-LacZ* embryo. Red arrowheads point to positive X-gal staining in the atrial tissue. Note that the staining is excluded from the SAN (circled in red). RSVC, right superior vena cava. SAN, sinoatrial node. Scale bars: 50 μm.

Figure 2

Figure 2. *Gja5-eh* enhancer activity recapitulates endogenous *Gja5* expression in *Nkx2-5*$^{+}$ myocardium, and is dependent on Nkx2-5 but is inhibited by Shox2.

(A-D) Triple immunofluorescent staining (Nkx2-5, Cx40, β-gal) on right atrium (A,B) and right ventricle (C,D) of the *Gja5-eh-LacZ* hearts at E12.5 and P60. CA, coronary arteries; VT, ventricular trabeculae; SAN, sinoatrial node. Scale bars: 100 μm. Also see Fig. S2. (E-J) *Gja5-eh-LacZ* transgenic mice were crossed onto *Nkx2-5*$^{+/+}$ (E-G) and *Nkx2-5*$^{Cre/Cre}$ (H-J) backgrounds and enhancer activity was examined by whole-mount X-gal staining and fluorescent immunostaining for β-galactosidase at E10.5. Scale bars: 50 μm. (K-R) *Gja5-eh-LacZ* transgenic mice were crossed onto *Shox2*$^{+/Cre}$;*ROSA26*$^{mTmG/mTmG}$ (K-N) and *Shox2*$^{Cre/Cre}$;*ROSA26*$^{mTmG/mTmG}$ (O-R) backgrounds, and examined at E13.5 for expression of Nkx2-5, mGFP and β-galactosidase by triple fluorescent immunostaining. Blue arrowheads point to ectopic β-gal signal co-localized with Nkx2-5 and mGFP in the SAN junction domain. RSVC, right superior vena cava; Sh, SAN head; Sj, SAN junction. Scale bars: 50 μm.

bioRxiv preprint doi: https://doi.org/10.1101/2020.05.07.083170; this version posted July 6, 2020. The copyright holder for this preprint (which was not certified by peer review) is the author/funder. All rights reserved. No reuse allowed without permission.

Figure 3

Figure 3. *Gja5-S1* and *Gja5-S2* are essential for myocardial *Gja5* expression.

(A, B) Schematic overview of CRISPR/Cas9-mediated mouse genome editing and generation of *Gja5*$^{\Delta 14}$ and *Gja5*$^{\Delta 12}$ alleles. (C-H) Double fluorescent immunostaining of Cx40 and Hcn4 on *Gja5*$^{+/+}$ (C, F), *Gja5*$^{\Delta 14/\Delta 14}$ (D, G), and *Gja5*$^{\Delta 12/\Delta 12}$ (E, H) hearts at P0. White/yellow arrowheads pointed regions are highlighted in white/yellow outlined squares as inserts. SAN, sinoatrial node; VT, ventricular trabeculae; CA, coronary arteries. Scale bars: 250 μm. (I) Western blot of Cx40 and GAPDH on protein extracts from atria or ventricles of *Gja5*$^{+/+}$ and *Gja5*$^{\Delta 14/\Delta 14}$ hearts at P0. (J) RT-qPCR detecting *Gja5* and *Gapdh* expression on atria or ventricles of *Gja5*$^{+/+}$ and *Gja5*$^{\Delta 14/\Delta 14}$ hearts at P0. Maximum *Gja5* expression relative to *Gapdh* is set as one. ****: $P < 0.0001$. Biological replicates N = 3.

Figure 4

Figure 4. Nkx2-5 mediates the interaction between *Gja5-S1*/*Gja5-S2* and the *Gja5* promoter.

(A) Relative positions of primer sets used for 3C assays. (B) Relative interaction frequency (RIF) in 3C assay between a combination of forward and reverse primer sets in E10.5 hearts of wild type and *Nkx2-5*$^{Cre/Cre}$ mice. Maximum RIF is set as one and relative fold changes are shown. ****: $P < 0.0001$. Biological replicates N = 3. (C) a schematic model proposing that *Gja5-S1* and *Gja5-S2* act in conjugation as a myocardial-specific *Gja5* distal enhancer by interacting with the *Gja5* promoter, and the enhancer activity depends on Nkx2-5 but inhibited by Shox2.

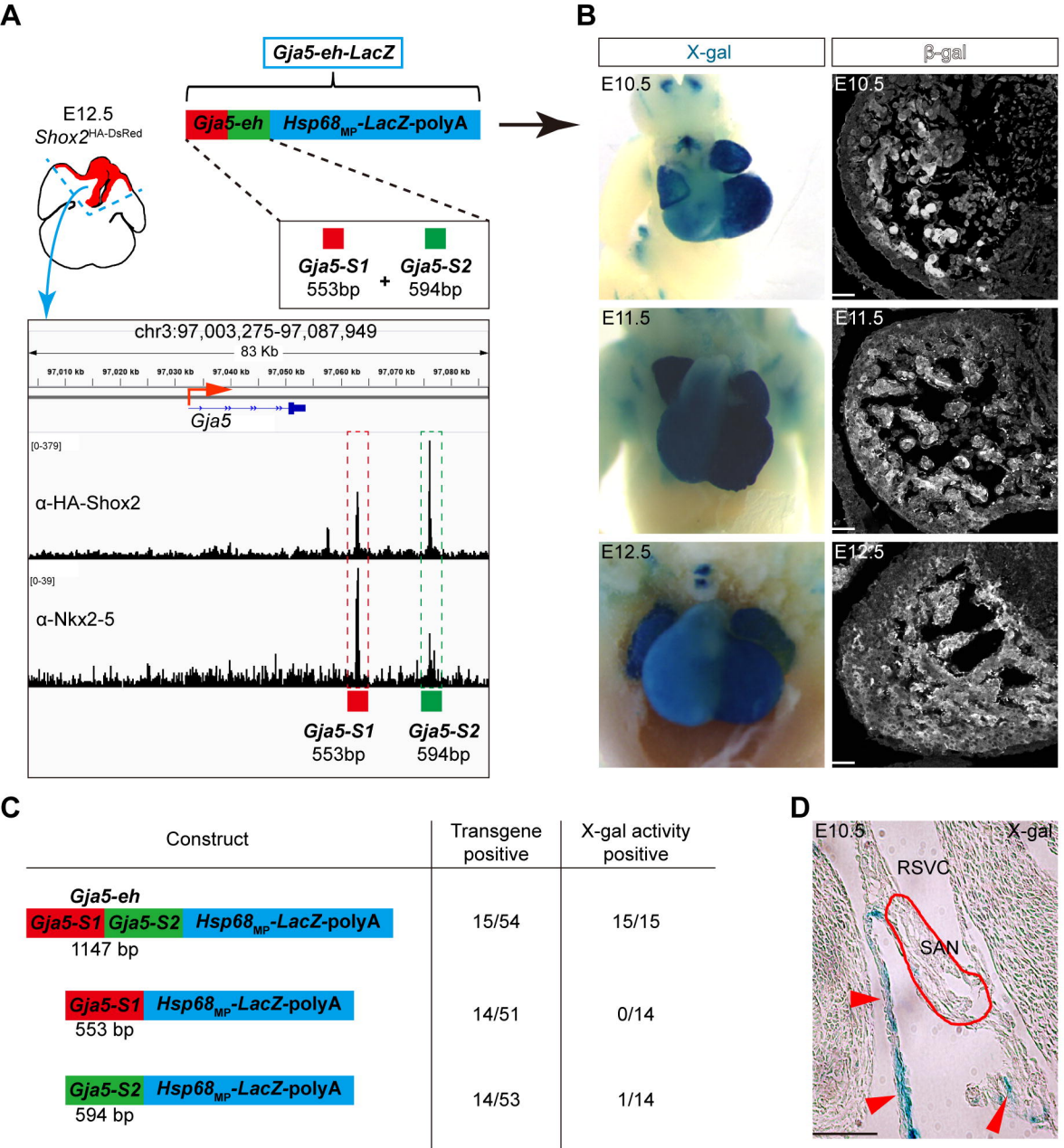
A
Gja5-eh-LacZ
Gja5-eh
Hsp68MP-LacZ-polyA
E12.5
Shox2HA-DsRed
Gja5-S1
553bp
+
Gja5-S2
594bp
chr3:97,003,275-97,087,949
83 Kb
97,010 kb
97,020 kb
97,030 kb
97,040 kb
97,050 kb
97,060 kb
97,070 kb
97,080 kb
Gja5
[0-379]
α-HA-Shox2
[0-39]
α-Nkx2-5
Gja5-S1
553bp
Gja5-S2
594bp
B
X-gal
β-gal
E10.5
E10.5
E11.5
E11.5
E12.5
E12.5
C
Construct
Transgene positive
X-gal activity positive
Gja5-eh
Gja5-S1
Gja5-S2
Hsp68MP-LacZ-polyA
1147 bp
15/54
15/15
Gja5-S1
Hsp68MP-LacZ-polyA
553 bp
14/51
0/14
Gja5-S2
Hsp68MP-LacZ-polyA
594 bp
14/53
1/14
D
E10.5
X-gal
RSVC
SAN

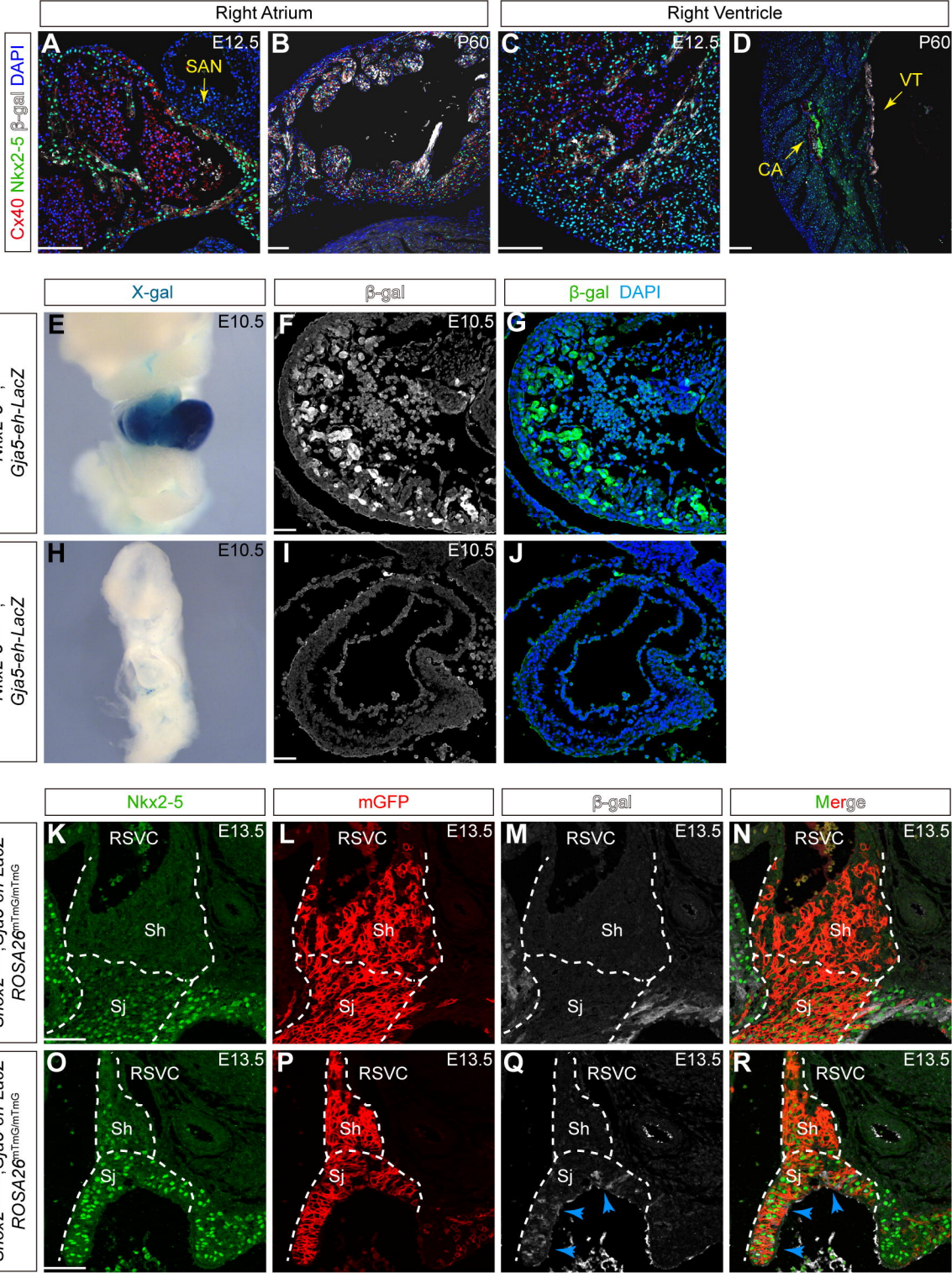
Right Atrium
Right Ventricle
Cx40 Nkx2-5 β-gal DAPI
A
E12.5
SAN
B
P60
C
E12.5
D
P60
VT
CA
X-gal
β-gal
β-gal DAPI
Nkx2-5+/+; Gja5-eh-LacZ
E
E10.5
F
E10.5
G
Nkx2-5Cre/Cre; Gja5-eh-LacZ
H
E10.5
I
E10.5
J
Nkx2-5
mGFP
β-gal
Merge
Shox2+/Cre; Gja5-eh-LacZ ROSA26mTmG/mTmG
K
RSVC
E13.5
Sh
Sj
L
M
N
Shox2Cre/Cre; Gja5-eh-LacZ ROSA26mTmG/mTmG
O
P
Q
R

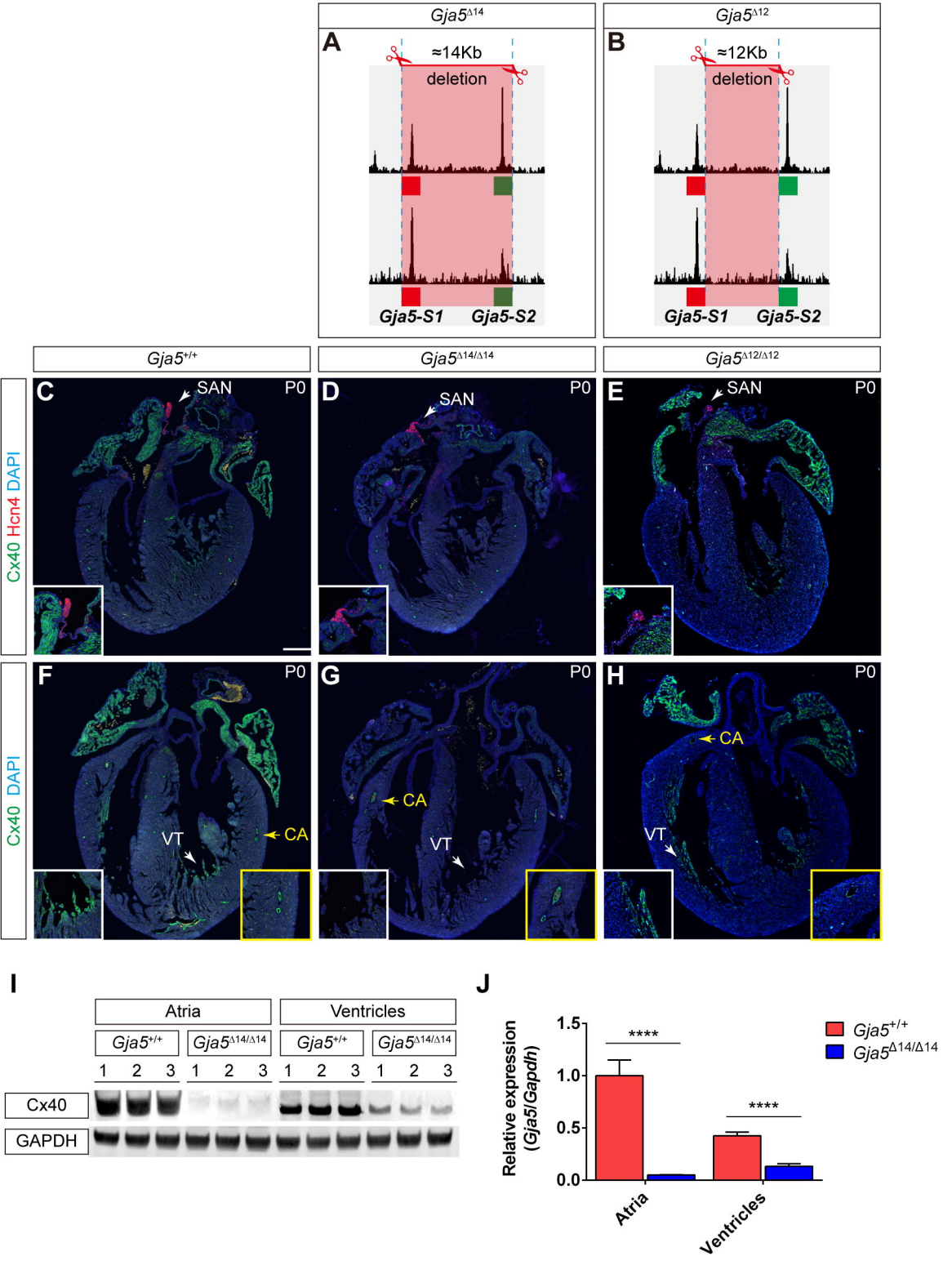
Gja5Δ14
Gja5Δ12
A
≈14Kb
deletion
Gja5-S1
Gja5-S2
B
≈12Kb
deletion
Gja5-S1
Gja5-S2
Gja5+/+
Gja5Δ14/Δ14
Gja5Δ12/Δ12
Cx40 Hcn4 DAPI
C
SAN
P0
D
SAN
P0
E
SAN
P0
Cx40 DAPI
F
P0
VT
CA
G
P0
CA
VT
H
P0
CA
VT
I
Atria
Ventricles
Gja5+/+
Gja5Δ14/Δ14
Gja5+/+
Gja5Δ14/Δ14
1 2 3 1 2 3 1 2 3 1 2 3
Cx40
GAPDH
J
Relative expression (Gja5/Gapdh)
1.5
1.0
0.5
0.0
****
****
Atria
Ventricles
Gja5+/+
Gja5Δ14/Δ14

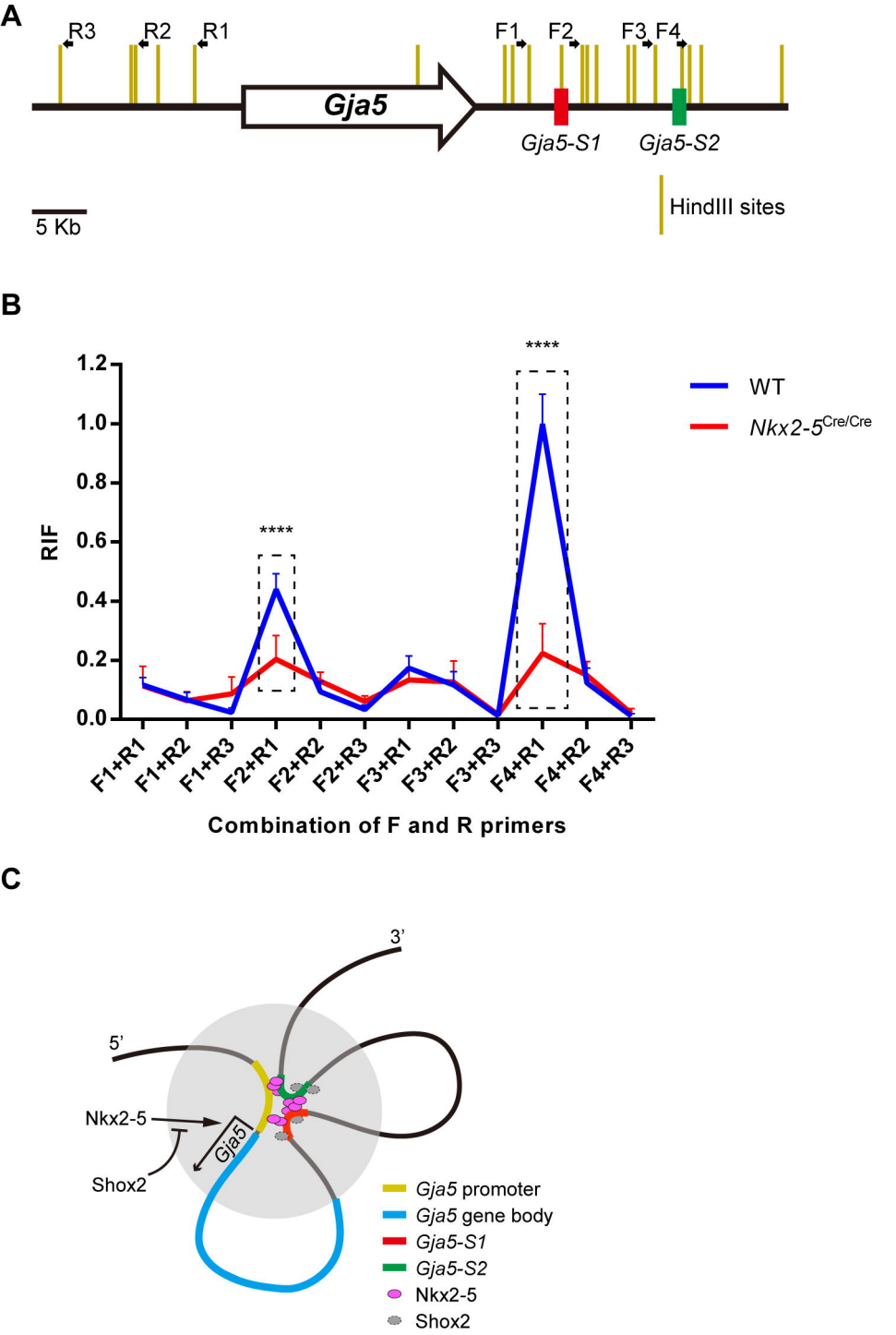
A
R3
R2
R1
F1
F2
F3
F4
Gja5
Gja5-S1
Gja5-S2
5 Kb
HindIII sites
B
****
****
1.2
1.0
0.8
0.6
0.4
0.2
0.0
RIF
WT
Nkx2-5Cre/Cre
F1+R1
F1+R2
F1+R3
F2+R1
F2+R2
F2+R3
F3+R1
F3+R2
F3+R3
F4+R1
F4+R2
F4+R3
Combination of F and R primers
C
3'
5'
Nkx2-5
Shox2
Gja5
Gja5 promoter
Gja5 gene body
Gja5-S1
Gja5-S2
Nkx2-5
Shox2